Available online at www.sciencedirect.com
SCIENCE DIRECT®
Physica E 18 (2003) 7–10
PHYSICA E
www.elsevier.com/locate/physe

Towards quantum electrical circuits

D. Vion, A. Aassime, A. Cottet, P. Joyez, H. Pothier, M.H. Devoret[1], C. Urbina, D. Esteve*

Quantronics Group, Service de Physique de l'Etat Condensé (DSM), CEA-Saclay, 91191 Gif-sur-Yvette, France

Abstract

Electrical circuits can behave quantum mechanically when decoherence induced by uncontrolled degrees of freedom is sufficiently reduced. Recently, different nanofabricated superconducting circuits based on Josephson junctions have achieved a degree of quantum coherence sufficient to allow the manipulation of their quantum state with NMR-like techniques. Because of their potential scalability, these quantum circuits are presently considered for implementing quantum bits, which are the building blocks of the proposed quantum processors. We have operated such a Josephson qubit circuit in which a long coherence time is obtained by decoupling the qubit from its readout circuit during manipulation. We report pulsed microwave experiments which demonstrate the controlled manipulation of the qubit state.

Keywords: Josephson effect; Quantum bits; Quantum coherence

1. Superconducting quantum circuits

Although quantum mechanics was developed to explain the properties of microscopic systems like electrons in atoms, its formalism treats all degrees of freedom, microscopic or macroscopic, on the same footing.

Why macroscopic objects usually do not display quantum effects is simply due to their large number of degrees of freedom and to the strong decoherence induced by their environment. However, nothing forbids a macroscopic system to behave quantum mechanically when its microscopic degrees of freedom are tied together to form a few collective ones, which are furthermore decoupled enough from the outside world. This was clearly proven in the eighties by the observation of tunneling, clearly a quantum property, for the phase difference across a Josephson junction [1]. The direct spectroscopy of quantum levels in various junction circuits further proved that superconducting electrical circuits can indeed behave quantum mechanically [1,2]. The general interest in quantum circuits raised in the nineties, with the advent of quantum computing algorithms. The discovery of a quantum factorisation algorithm, and subsequently of quantum error-correcting codes proved that quantum processors could perform tasks beyond reach of usual computers whatever their speed gains in the future (see Ref. [3] for a general review). A quantum processor consists of an assembly of two-level systems, called quantum bits, which can be independently manipulated and readout, and whose interactions can be varied at will in order to perform logic operations.

Among the various physical systems considered for implementing quantum bits, electrical circuits are appealing because of their potential scalability. Various Josephson circuits have in particular been investigated. Their relative advantages and drawbacks are mainly determined by their sensitivity to uncontrolled noise sources which dominate decoherence, and by the fidelity and back-action of their measuring circuit. Josephson qubits can be classified according to the nature of the degree of freedom involved, as shown by the following examples.

In current-biased junctions with a large capacitance ($\approx$1–10 pF), this degree of freedom is the phase difference across the junction. At bias currents close to the critical current, the energy spectrum is anharmonic, and the two lowest energy states form a "phase"-qubit. Quantum tunneling to the

* Corresponding author.
E-mail address: desteve@cea.fr (D. Esteve).
[1] Present address: Applied Physics, Yale University, New Haven, CT 06520, USA.

1386-9477/03/$ - see front matter © 2003 Elsevier Science B.V. All rights reserved.
doi:10.1016/S1386-9477(02)00933-5

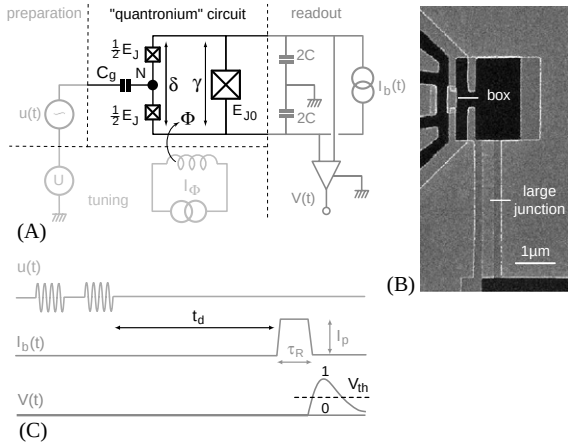

Fig. 1. (A) Idealized circuit diagram of the "quantronium", with its tuning, preparation and readout blocks. (B) Scanning electron micrograph of a sample. (C) Manipulation and readout signals: microwave pulses $u(t)$ applied to the gate manipulate the quantum state of the circuit. Readout is performed by applying a current pulse $I_b(t)$ to the large junction and by monitoring the voltage $V(t)$ across it.

voltage-state provides the readout, and decoherence is due to noise in the control parameters such as the bias-current. Quantum state manipulation can be achieved by injecting a resonant microwave current in the junction [4,5].

"Flux"-qubits [6] have been implemented in small superconducting loops interrupted by one or more intermediate-capacitance junctions ($\approx$ 100 fF). The qubit levels correspond to different flux-states of the loop, and the readout is performed by measuring the flux through the loop with a SQUID. Decoherence is due to flux-noise through the loop, and to the back-action of the measuring SQUID. Manipulation of the qubit state is performed by applying an AC field through the qubit loop. Finally, the charge states of a small island connected to a superconducting reservoir by an ultrasmall capacitance junction ($\approx$1 fF) also provide a qubit [7]. When the Josephson energy is small enough, the two lowest energy states are formed with the charge states differing by a single Cooper pair in the island. In this circuit, called the Cooper pair box, superpositions of the "charge"-qubit states have been produced by inducing a sudden non-adiabatic evolution of the hamiltonian [8]. The coherence time, of the order of a few ns, is limited by the island charge noise, which directly affects the qubit transition frequency, and by the back-action of the measuring apparatus.

2. The quantronium

The quantronium circuit [9,10] described in Fig. 1 consists of a superconducting loop interrupted by two adjacent small Josephson tunnel junctions with capacitance $C_j/2$ and Josephson energy $E_J/2$ each, which define a low capacitance C_Σ superconducting electrode called the "island", and by a large Josephson junction with large Josephson energy ($E_{J0} \approx 20E_J$). The island is biased by a voltage source U through a gate capacitance C_g. In addition to E_J, the quantronium has a second energy scale which is the Cooper pair Coulomb energy $E_C = (2e)^2/2C$.

This system has discrete quantum states which are in general quantum superpositions of several charge states with different number $\hat{N}$ of excess Cooper pairs in the island, and which carry different currents around the loop. The eigenstates and eigenenergies are determined by the dimensionless gate charge $N_g = C_g U/2e$, the phase $\delta = \gamma + \phi$, where γ is the phase across the large junction and $\phi = \Phi/\varphi_0$, with Φ the external flux imposed through the loop and $\varphi_0 = \hbar/2e$. The bias current I_b is zero except during readout of the state. In this device $E_J \simeq E_C$ and neither $\hat{N}$ nor its conjugated variable $\hat{\theta}$ is a good quantum number. In contrast, the large junction is shunted by a large capacitor C so that γ is almost a classical variable. In this regime, the energy spectrum is sufficiently anharmonic for the two lowest energy states $|0\rangle$ and $|1\rangle$ to form a two-level system. This system corresponds to an effective spin one-half with eigenstates $|0\rangle \equiv |s_z = +1/2\rangle$ and $|1\rangle \equiv |s_z = -1/2\rangle$. At $N_g = 1/2$, $I_b = 0$ and $\phi = 0$, its "Zeeman energy" $h\nu_{01}$, of the order of E_J, is stationary with respect to N_g, I_b and ϕ [9], making the system immune to first-order fluctuations of the control parameters. Manipulation of the quantum state is thus performed at this optimal point by applying microwave pulses $u(t)$ with frequency $\nu \simeq \nu_{01}$ to the gate, and any superposition $|\Psi\rangle = \alpha|0\rangle + \beta|1\rangle$ can be prepared, starting from $|0\rangle$.

For readout, we have implemented a strategy reminiscent of the Stern et Gerlach experiment: the information about the quantum state of the quantronium is transferred onto another variable, the phase γ, and the two states are discriminated through the supercurrent in the loop [10]. For this purpose, a trapezoidal readout pulse $I_b(t)$ with a peak value slightly below the critical current $I_0 = E_{J0}/\varphi_0$ is applied to the circuit. When starting from $\langle\delta\rangle \approx 0$, the phases $\langle\gamma\rangle$ and $\langle\delta\rangle$ grow during the current pulse, and consequently a state-dependent supercurrent develops in the loop. This current adds to the bias-current in the large junction, and by precisely adjusting the amplitude and duration of the $I_b(t)$ pulse, the large junction switches during the pulse to a finite voltage state with a large probability p_1 for state $|1\rangle$ and with a small probability p_0 for state $|0\rangle$ [10]. The efficiency of this projective measurement is expected to exceed $\eta = p_1 - p_0 = 0.95$ for optimum readout conditions. The readout part of the circuit was tested by measuring the switching probability p as a function of the pulse height I_p, for a current pulse duration of $\tau_r = 100$ ns, at thermal equilibrium. The discrimination efficiency was then estimated using the calculated difference between the currents of both $|0\rangle$ and $|1\rangle$ states. Its value $\eta = 0.6$ is lower than the expected one, possibly due to noise coming from the large bandwidth current-biasing line. An actual "quantronium" sample is shown on the right side of Fig. 1. It

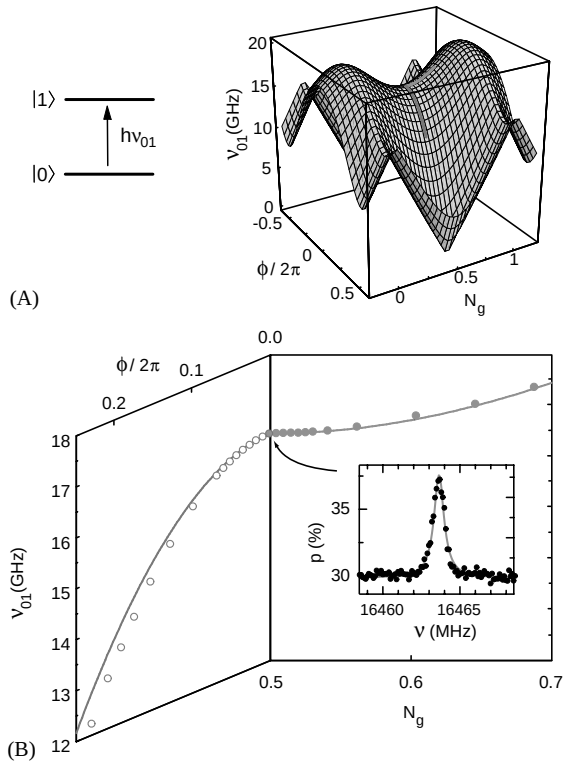

Fig. 2. (A) Calculated transition frequency v_{01} as a function of ϕ and N_g. (B) Measured center transition frequency (symbols) as a function of reduced gate charge N_g for reduced flux $\phi = 0$ (right panel) and as a function of ϕ for $N_g = 0.5$ (left panel), at 15 mK. Spectroscopy is performed by measuring the switching probability p (10^5 events) when a continuous microwave irradiation of variable frequency is applied to the gate before readout. Continuous line: best fits used to determine circuit parameters. Inset: Narrowest line shape, obtained at the saddle point (Lorentzian fit with a FWHM $\Delta v_{01} = 0.8$ MHz).

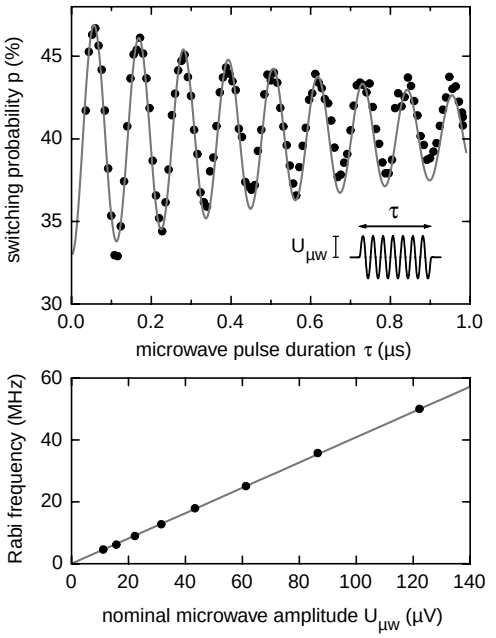

Fig. 3. Top: Rabi oscillations of the switching probability p (5×10^4 events) measured just after a resonant microwave pulse of duration τ. Solid line is a fit used to determine the Rabi frequency. Bottom: test of the linear dependence of the Rabi frequency with $U_{\mu w}$.

was fabricated by aluminum deposition through a suspended mask patterned by e-beam lithography. The switching of the large junction to the voltage state is detected by measuring the voltage across it with an amplifier at room temperature. By repeating the experiment (typically a few 10^4 times), the switching probability is measured, which gives the weights of both states.

Spectroscopic measurements of v_{01} were performed by applying to the gate a weak continuous microwave irradiation suppressed just before the readout current pulse. The variations of the switching probability as a function of the irradiation frequency display a resonance whose center frequency evolves as a function of the DC gate voltage and flux as predicted, reaching $v_{01} \simeq 16.5$ GHz at the optimal working point (see Fig. 2). These spectroscopic data allow to determine the relevant circuit parameters: $i_0 = 18.1$ nA and $E_J/E_C = 1.27$. At the optimal working point, the line width was found to be minimal with a 0.8 MHz FWHM, corresponding to a quality factor $Q = 2 \times 10^4$. Close to the optimal point, controlled rotations of the spin could be performed using large amplitude microwave pulses. Prior to readout, a single pulse at the transition frequency with variable amplitude $U_{\mu w}$ and duration τ was applied. The resulting change in switching probability is an oscillatory function of the product $U_{\mu w}\tau$ (see Fig. 3), in agreement with the theory of Rabi oscillations. The linear dependence of the Rabi frequency on the microwave amplitude was used to calibrate the rotation angle. It can be seen that the amplitude of the Rabi oscillations is smaller than the estimated efficiency. This loss of contrast is possibly due to a relaxation of the level population during the measurement itself.

The measurement of the coherence time during free evolution was obtained using a two-pulse sequence with a delay Δt during which the spin evolves freely. For a given detuning Δv of the microwave frequency, the switching probability displays decaying oscillations of frequency Δv (see Fig. 4), which correspond to the "beating" of the spin precession with the external microwave field. This experiment is analogous to the Ramsey-fringe experiment. The envelope of the oscillations yields the coherence time $T_\varphi \simeq 0.5$ μs, which corresponds to 8000 coherent free precession turns on average. This time is shorter than the relaxation time $T_1 = 1.8$ μs deduced from the exponential decay of the the switching probability when the readout is delayed after a single pulse. Decoherence of the quantum state is thus dominated by dephasing and not by relaxation from the excited state to the ground state.

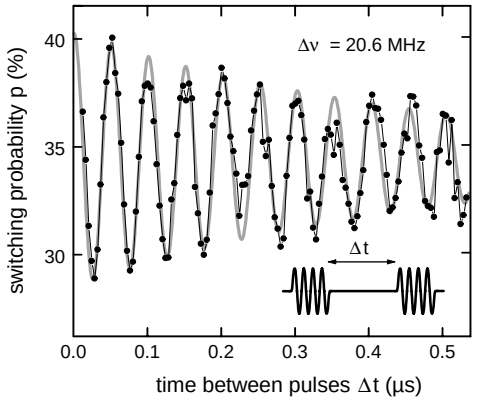

Fig. 4. Switching probability after a two-pulse sequence as a function of the pulse delay, at $N_g = 0.50$, $\phi = 0$ and $\Delta\nu = 20.6$ MHz. The decay time constant is $T_\varphi \sim 500$ ns.

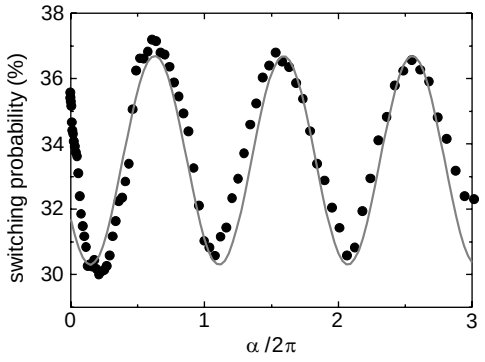

Fig. 5. Switching probability following a two-pulse sequence as a function of the rotation angle α induced by a bias-current pulse with variable amplitude. The 100 ns bias-current pulse is applied between the two microwave pulses. The sinusoidal solid line is a guide for the eye.

When departing from the optimal point, the coherence time T_φ decreases rapidly. By inserting a π pulse in the middle of a two-pulse sequence, NMR-like echo experiments can be performed to probe the spectral density of the noise sources [11]. In this sequence, the random phases accumulated during the two free-evolutions compensate if the transition frequency does not change on this time scale. When the charge noise dominates the line width, the observation of echoes indicates that fluctuations with a characteristic frequency below 1 MHz mostly contribute. When the phase-noise dominates, the absence of echoes, on the contrary, points toward fluctuations with a higher characteristic frequency.

At the optimal point, the two-pulse sequence can be used to test the phase-shift between both qubit states induced by a small change of the bias-current during a short time, as shown in Fig. 5. Microwave pulses and bias-current pulses provide a complete set of single qubit operations. Mastering the quantum evolution of an individual qubit is a first step towards functional quantum circuits. It is, however, still necessary to improve the coherence time by about 100, to achieve high fidelity readout, and to implement flexible qubit interactions. Coupling several quantronium circuits can in principle be achieved using on-chip capacitors and/or ultrasmall junctions, and coupling schemes have been proposed for all Josephson qubits. Logic gate operation could then be probed by measuring quantum correlations in entangled multi-qubit states. In view of all the recent developments in the area of Josephson qubits, elementary quantum processors can be envisioned.

The essential technical contribution of Pief Orfila and the support from the IST-10673 SQUBIT contract, and from CNRS are gratefully acknowledged.

References

[1] M.H. Devoret, D. Esteve, C. Urbina, J.M. Martinis, A.N. Cleland, J. Clarke, in: Y. Kagan, A.J. Leggett (Eds.), Quantum Tunneling in Condensed Media, Elsevier, Amsterdam, 1992.
[2] Siyuan-Han, R. Rouse, J.E. Lukens, Phys. Rev. Lett. 84 (2000) 1300.
[3] M.A. Nielsen, I.L. Chuang, Textit Quantum Computation and Quantum Information, Cambridge University Press, Cambridge, 2000.
[4] Siyuan Han, Yang Yu, Xi Chu, Shih-I Chu, Zhen Wang, Science 296 (2002) 889.
[5] J.M. Martinis, S. Nan, J. Aumentado, C. Urbina, Phys. Rev. Lett. 89 (2002) 117901.
[6] C.H. van der Wal, A.C.J. ter Haar, F.K. Wilhelm, R.N. Schouten, C.J.P.M. Harmans, T.P. Orlando, S. Lloyd, J.E. Mooij, Science 290 (2000) 773.
[7] V. Bouchiat, D. Vion, P. Joyez, D. Esteve, M.H. Devoret, Phys. Scripta T 76 (1998) 165.
[8] Y. Nakamura, C.D. Chen, J.S. Tsai, Phys. Rev. Lett. 79 (1997) 2328;
Y. Nakamura, Yu.A. Pashkin, J.S. Tsai, Nature 398 (1999) 786;
Y. Nakamura, Yu.A. Pashkin, T. Yamamoto, J. S. Tsai, Phys. Rev. Lett. 88 (2002) 047901.
[9] D. Vion, A. Aassime, A. Cottet, P. Joyez, H. Pothier, C. Urbina, D. Esteve, M.H. Devoret, Science 296 (2002) 886.
[10] A. Cottet, D. Vion, P. Joyez, A. Aassime, D. Esteve, M.H. Devoret, Physica C 367 (2002) 197.
[11] D. Vion, A. Aassime, A. Cottet, P. Joyez, H. Pothier, C. Urbina, D. Esteve, M.H. Devoret, Phys. Ser. T 102 (2002) 162.